



HAL
open science

Room temperature ionic liquids to tailor resorcinol-formaldehyde polymer gels

Balázs Nagy, Erik Geissler, Krisztina Laszlo

► **To cite this version:**

Balázs Nagy, Erik Geissler, Krisztina Laszlo. Room temperature ionic liquids to tailor resorcinol-formaldehyde polymer gels. *Microporous and Mesoporous Materials*, 2020, 294, pp.109888. hal-02447713

HAL Id: hal-02447713

<https://hal.science/hal-02447713>

Submitted on 21 Jan 2020

HAL is a multi-disciplinary open access archive for the deposit and dissemination of scientific research documents, whether they are published or not. The documents may come from teaching and research institutions in France or abroad, or from public or private research centers.

L'archive ouverte pluridisciplinaire **HAL**, est destinée au dépôt et à la diffusion de documents scientifiques de niveau recherche, publiés ou non, émanant des établissements d'enseignement et de recherche français ou étrangers, des laboratoires publics ou privés.

Room temperature ionic liquids to tailor resorcinol – formaldehyde polymer gels

Balázs Nagy¹, Erik Geissler², Krisztina László^{1*}

¹Department of Physical Chemistry and Materials Science, Budapest University of Technology and Economics, H-1521 Budapest, PO Box 91, Hungary

² Université Grenoble Alpes, CNRS, LIPhy, 38000 Grenoble, France

Abstract

Synthesis of resorcinol – formaldehyde polymer gels was studied in various room temperature ionic liquid (RTIL) – water mixtures. Low temperature nitrogen adsorption observations reveal that the size of both the anions and of the cations influences the pore morphology of the aerogel. The 1-ethyl-3-methylimidazolium ethyl sulphate ionic liquid (IL) on its own is also able to catalyse the synthesis, yielding a totally metal free carbon aerogel precursor. The effect of water content on the gel structure is striking, thereby also offering a means of systematically adjusting the apparent surface area, the width of the pore entrance and the volume of the pores detectable by nitrogen. Here, the nature of the gel synthesis itself depends sensitively on the intrinsic pH, which is influenced by the anion of the IL. Comparison of these findings with published molecular dynamics simulations shows that the morphology of the gels is correlated with the structure of the mixed water – IL solvent, which also tunes the concentration of the IL catalyst.

Keywords: ionogel, polymer aerogel, ionic liquid, binary solvent, imidazolium cation

1. Introduction

Porous polymers, either as monoliths or particles of various sizes, have recently attracted increased attention. Applications of such materials are not limited merely to the construction industry, chromatographic separation or catalyst supports, but can also be used in gas storage materials, membranes, in biological and electronic devices, and possibly as precursors of nanostructured carbon materials [1]. Recently, supermacroporous polymer gels opened a new avenue of application, particularly if supermacroporosity is coupled with other exclusive features of the polymer matrix or its surface [2, 3]. Responsive porous polymers have enormous potential in a wide range of biomedical applications including targeted and/or controlled release or tissue engineering [4]. These high value applications are the focus of the

¹ Corresponding author. Department of Physical Chemistry and Materials Science, BME, H-1521, Budapest, Hungary.
E-mail address: klaszlo@mail.bme.hu (K. László).

the recent emphasis on developing reliable methods for preparing porous polymers with designed pore architectures as well as pore surface functionalities [5].

Polymer aerogels exhibit desirable physical properties such as excellent mass transfer, low density, limited thermal conductivity, sound velocity, and dielectric permittivity [6]. Since the first report of Pekala [7], sol-gel technology, which is the most versatile means of sculpting their porosity, has been widely used to synthesize organic porous materials with tuned pore texture. The flexibility of this method lies in its outstanding sensitivity to synthesis conditions both in the sol formation and the gelation phases. Already the choice of solvent, i.e., the porogen itself, offers versatile potential tuning tools in the gelation through its protic/aprotic nature, dipole moment or viscosity. The overall morphology depends greatly on the solvation, as well as on the composition, of the monomers and porogens in the polymerization mixture, since the porous structure is born in the phase separation of the rigid polymer from the porogen [6, 8]. An additional tool in the box of tuning parameters is the means of solvent removal, which can yield cryo-, aero- or xerogels [9]. Although in most cases these gels are prepared from resorcinol and formaldehyde precursors, other phenolic molecules, comonomers or incorporated nanoparticles are often used to tune the chemistry of the polymer and obtain carbons with more advantageous surface chemical composition [6, 10, 11].

Room temperature ionic liquids (RTILs), which typically consist of a bulky organic cation paired with an inorganic or organic anion at room temperature, have attracted considerable attention because of their unique properties, such as nonflammability, negligible volatility, high ionic conductivity and thermal stability [12]. They are fundamentally exciting materials, but their high cost limits technological applications [13].

Although in recent years, RTILs have been used in polymer science, mainly as polymerization media in several types of polymerization processes [14, 15], studies on resorcinol – formaldehyde polymer systems have not been reported. The closest analogue was described by Ogoshi et al. [16]. These authors prepared ionic liquid - phenol resin hybrids by an “in situ” method that involves initial polymerization of phenol and formaldehyde, followed by simultaneous cross-linking between phenol polymer chains using para-toluenesulfonic acid in 1-ethyl-3-methylimidazolium bis(trifluoromethanesulfonyl)amide. This procedure results in highly ion-conductive ionic liquid - phenolic resin hybrids. Imidazolyl-functionalized ordered mesoporous polymers can be synthesized in a single step by taking advantage of the self-assembly of 4-(imidazole-1-yl)phenol-phenol-formaldehyde precursors [17]. Furthermore, only a limited number of publications report the use of room temperature ionic solvents in the synthesis of carbon aerogels. The role of the ionic liquids (ILs) here can be

manifold: they can be media, solvents, soft templates during the formation of carbon materials or their precursors, or even carbon and/or heteroatom sources [18, 19, 20]. ILs may also serve as catalysts. Imidazolium-based ILs linked to an FDU-type mesoporous polymer successfully fostered the cycloaddition of CO₂ with various epoxides [21]. Metal containing 1-butyl-3-methylimidazolium tetrachloroferrate(III) has also been employed as a good catalyst and solvent for the efficient conversion of sugars into 5-hydroxymethylfurfural [22]. Nitrogen- or boron containing ionic liquids were found to be ideal precursors, not only for nitrogen or boron doped carbon materials [23, 24, 25, 26], but also in various structural carbon and silica composites [27, 28]. In spite of these efforts in carbon aerogel studies, no systematic work has been reported on the polymer precursor itself.

The present investigation is intended to shed light on the capacity of RTILs to tune the pore morphology of porous resorcinol – formaldehyde based polymers. In gel formation, particularly during the early stages where elastic forces are weak, the architecture of the gel responds to the thermodynamic state and local organisation of the solvent molecules.

To study the effect of the constituent ions, RTILs composed of various methyl-imidazolium cations with acetate, methyl- and ethyl-sulphate anions were used as co-solvents with water. As several properties of the ILs (e.g., density, viscosity, polarity, or conductivity) can change drastically in the presence of small amounts of other substances, notably water [12, 29, 30, 31, 32], we systematically study the influence of water content on the textural morphology of the organic resorcinol - formaldehyde aerogel. To detect these effects, only scanning electron microscopy (SEM) imaging and low temperature nitrogen adsorption techniques were used, since the resulting polymers tend to collapse when immersed in liquid, or on being exposed to the external pressures employed in mercury porosimetry.

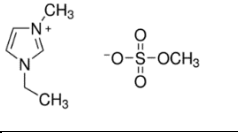
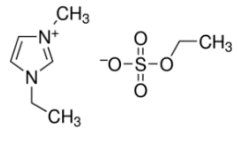
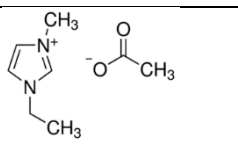
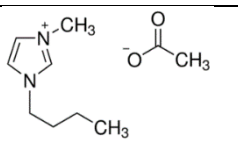
2. Experimental

2.1. Synthesis

Samples were prepared by the sol-gel technique. Resorcinol (R) was dissolved in 3 mL of the selected ionic solvent, then formaldehyde (F, 37% aq. solution) and Na₂CO₃ catalyst (C) were added. The concentration of R in the initial solution was 0.14 g/mL, with R/F and R/C molar ratios 0.5 and 50 respectively. The initial sol was prepared at 70 °C, sealed in a glass vial and cured at 85 °C for 7 days. Polymer liogels were also synthesized in water (1) - 1-ethyl-3-methylimidazolium ethyl sulphate (2) binary solvents with a systematically set ratio and without addition of Na₂CO₃. The IL was removed from the resulting gels by water extraction

and the water was then replaced by acetone, which in turn was removed by supercritical carbon dioxide (scCO₂) extraction. The ILs employed are listed in Table 1.

Table 1 Room temperature ionic liquids used as synthesis medium

Name	Acronym	Formula	Molar mass	Density
				g/cm ³
1-Ethyl-3-methylimidazolium methyl sulphate	[emim][MeSO ₄]		222.26	1.286 ^{25 °C} [33]
1-Ethyl-3-methylimidazolium ethyl sulphate	[emim][EtSO ₄]		236.29	1.24100 ^{20°C} [29] 1.237 ^{25 °C} [33]
1-Ethyl-3-methylimidazolium acetate	[emim][Ac]		170.21	1.027 ^{25 °C} [34]
1-Butyl-3-methylimidazolium acetate	[bmim][Ac]		198.26	1.05 [35]

2.2. Methods

The morphology of the samples was investigated at different length scales using scanning electron microscopy (SEM) and low temperature gas adsorption techniques. SEM micrographs were obtained with a field emission SU8030 (Hitachi) instrument. Low temperature (-196 °C) nitrogen adsorption isotherms were measured by a NOVA 2000 (Quantachrome) automatic analyzer. The apparent surface area S_{BET} was calculated using the Brunauer–Emmett–Teller (BET) model. The micropore volume (W_0) was derived from the Dubinin–Radushkevich (DR) plot. Although pore size distributions in the narrower mesopores cannot be reliably deduced from Kelvin equation based methods, it is still accepted for comparative purposes. The Kelvin equation-based Barrett–Joyner–Halenda (BJH) model was used in this study, since the lack of kernel for polymers prevented the use of more advanced computational models. Transformation of all the primary adsorption data was performed by the Quantachrome software ASiQwin version 3.0.

3. Results and discussion

3.1. Ionic solvent as catalyst

The most frequently used catalyst in the sol/gel reaction of resorcinol and formaldehyde is Na_2CO_3 . Taylor et al. found that the (alkali) metal ions of the basic catalyst play an important role. They concluded that the presence of these metal ions is crucial in the gelation process and also that during the pre-gelation larger, more hydrated cations result in much larger cluster sizes [36]. It has, however, also been reported that RF polymer gels are synthesized with $(\text{NH}_4)_2\text{CO}_3$ as catalyst [37]. Here, by contrast, we report that some ionic liquids can catalyse the reaction in the absence of any added catalyst.

Figure 1 compares samples synthesized with the same initial composition in ca. 10 wt% water containing [emim][EtSO₄], with and without Na_2CO_3 catalysis. The shapes of the isotherms as well as the deduced parameters (listed in **Table 2**), indicate that the texture of the two polymer aerogels, RFemimES (with Na_2CO_3) and RFemimES9 (without added catalyst) are very similar. Deviations occur only in the wider pore range, as reflected also in the 10 % increase of the total pore volume. The isotherms can be classified as Type IVa with a hysteresis loop of class H2a [38]. Although the morphology designated by this particular type of isotherm and hysteresis loop class will be discussed in detail later, here we merely state that the discrepancy between the pore size distributions deduced respectively from the adsorption and desorption branches is related to the complex pore network of the interconnected nonuniform pores. The region, and the size, of the pores that governs the filling (adsorption) and emptying (desorption) processes in the the pores is different and this is reflected in the Kelvin equation-based computation results.

To understand the role of the ionic liquid in the sol/gel synthesis of resorcinol – formaldehyde hydrogels, we recall the mechanism of the polymerization. The first step is an addition reaction between the resorcinol and formaldehyde, followed by condensation reactions leading to cross-linking. The reaction begins with deprotonation of R by the base catalyst (typically Na_2CO_3 , or occasionally other alkaline carbonates or hydroxides), or protonation of F (acidic conditions). In basic conditions the reaction between the phenoxide and formaldehyde in ortho- or para-positions results in hydroxymethylation of the resorcinol (addition reaction). Finally, polycondensation occurs. The gel structure itself is composed of clusters that develop from the growth of the oligomers. Generally, the pH ranges 1-4 or pH 5.5-7.5 are favoured for the synthesis. Reactions between resorcinol and formaldehyde at pH outside these ranges may produce precipitates but not porous gels [36, 39, 40, 41].

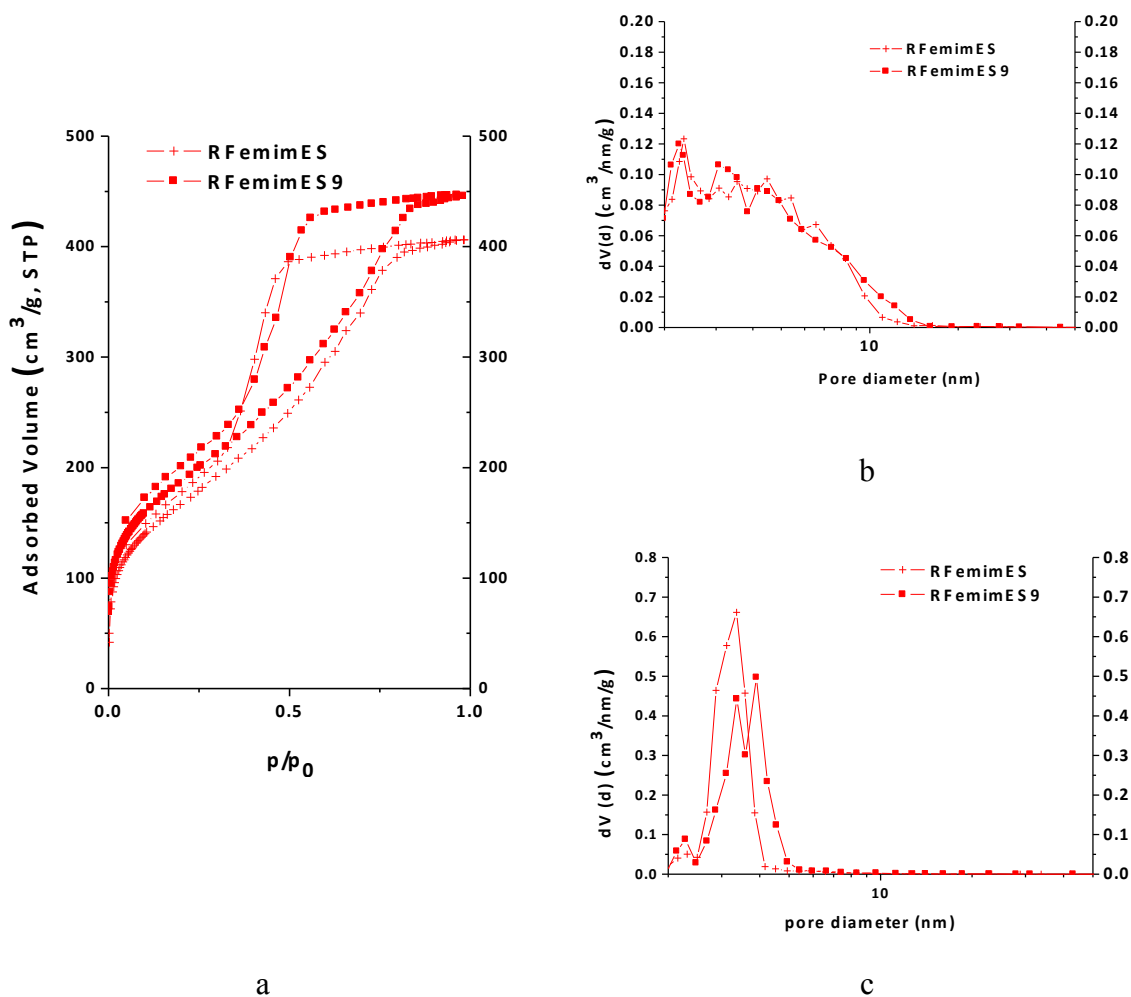


Figure 1 Low temperature (-196 °C) nitrogen adsorption/desorption isotherms (a) and pore size distribution from the adsorption (b) and desorption (c) branches of polymer aerogels synthesized in water - [emim][EtSO₄] mixture with and without Na₂CO₃ catalyst.

Table 2 Parameters deduced from low temperature nitrogen adsorption isotherms of polymer aerogels synthesized in aqueous [emim][EtSO₄] solvent with and without Na₂CO₃ catalysis (molar fraction of water in the initial water - [emim][EtSO₄] mixture was 0.57)

Sample acronym	Na ₂ CO ₃	$S_{\text{BET}}^{\text{a}}$	W_0^{b}	$V_{\text{tot}}^{\text{c}}$	$V_{\text{meso}}^{\text{d}}$	$d_{\text{SEM}}^{\text{e}}$
		m ² /g	cm ³ /g	cm ³ /g	cm ³ /g	nm
RFemimES	with	608	0.24	0.63	0.39	19 ± 3
RFemimES9	without	674	0.24	0.69	0.45	16 ± 3

^a Apparent surface area from BET, ^b Micropore volume from DR, ^c Pore volume at $p/p_0 \rightarrow 1$, ^d $V_{\text{tot}} - W_0$, ^e average diameter of the beads from SEM images (based on approx. 100 measurements)

Although a different type of investigation, which would lie outside the scope of this work, is needed to understand the mechanism of the RF gel formation in aqueous solutions of ionic liquids, it is nevertheless possible here to draw certain conclusions. RF based aerogels could be synthesized both in aqueous solutions of commercial [emim][MeSO₄] and [emim][EtSO₄] ILs but, notably, not in the acetates. This finding implies that the anion plays a crucial role in adjusting the conditions. In 100 g/L solution the pH of [emim][EtSO₄] is 8.2, while in both [emim][Ac] and [bmim][Ac] it is acidic, 5.4 and 6.1, respectively [34]. In the mixed solvent used in the synthesis of RFemimES9 the initial pH was 9.8, i.e., much higher than the usual pH value in the reactions under purely aqueous conditions. These observations imply that the basic condition of the [emim] alkyl sulfate medium is necessary to ensure gelation. When the acetate anion is present and the pH is thus acidic, only precipitates were formed, but no 3D network.

3.2. Comparison of the effect of various RTILs

A set of samples was prepared at relatively low water content (ca. 10 wt%), introduced by the aqueous formaldehyde solution. The ratio of additional water : IL was thus approximately 0 : 1 by volume (**Table 3**). All the ILs used were miscible with water and the starting reaction mixture was fully transparent.

The SEM images reveal the typical interconnected spherical structure of the RF polymer aerogels [9] (**Figure 2**). Although sample RFemES seems to be more compact than the others, the size of the elementary beads is not notably influenced by the IL selected (**Table 4**). While ILs are considered to be an inert medium, it has been found that imidazolium type ILs may participate in various chemical reactions [42]. When bases are present, the imidazolium ion is deprotonated and this nucleophile may react with electrophiles, like aldehydes. 1-Ethyl-3-methylimidazolium having BF₄ or PF₆ anion reacts with benzaldehyde in the presence of bases or if the anion is acetate in a Horner –Wadsworth – Emmons Reaction [43]. However, no such reaction has been reported in case of formaldehyde. Neither nitrogen nor sulphur atoms were detected by TG/MS analysis in the samples, which implies that neither the cations nor the anions were incorporated into the polymer.

Table 3 Acronym of the samples and initial water content of the precursor solution

Sample	Solvent	Water:IL	Initial water content	
acronym		V/V	Molar fraction	wt%

RFemimMS	[emim][MeSO ₄]	0:1	0.54	8.8
RFemimES	[emim][EtSO ₄]	0:1	0.57	9.1
RFemimAc	[emim][Ac]	0:1	0.62	10.2
RFbmimAc	[bmim][Ac]	0:1	0.56	10.4

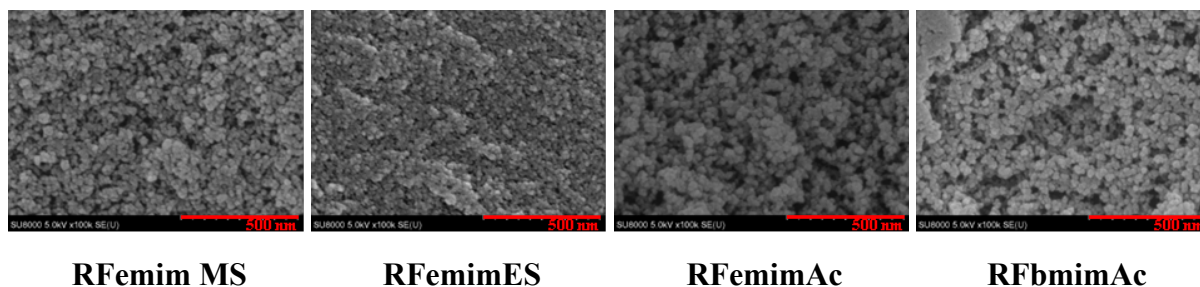


Figure 2 SEM micrographs of the polymer samples synthesized in different aqueous RTIL media.

The morphology was also probed by N₂ (size 0.35 nm) adsorption at 77 K. The adsorption isotherms together with the aerogel obtained in RTIL free conditions (sample RFw) are shown in **Figure 3 a-b**. For clarity they are grouped according to ionic composition.

All the nitrogen adsorption/desorption isotherms belong to Type IVa, as defined in the latest IUPAC classification [38], i.e., the initial monolayer-multilayer adsorption is later superseded by pore condensation. The hysteresis implies that the system contains pores wider than ~ 4 nm. As expected from the SEM images, the complex interconnected 3D network leads to hysteresis loops of Type H2a and H2b. With such pore morphology the desorption path is often subject to network effects and pore blocking. These phenomena occur if wide pores are connected to the external surface through narrow necks (ink-bottle shape). Thus, the shape of the desorption branch depends on the size and spatial distribution of the narrow outlets. The network empties at a relative pressure that corresponds to a characteristic percolation threshold. In such cases the pore size distribution deduced from the desorption branch provides useful information on the limiting neck size. The desorption branch of the isotherms was therefore used to deduce the pore size distribution (**Figure 3 c-d**).

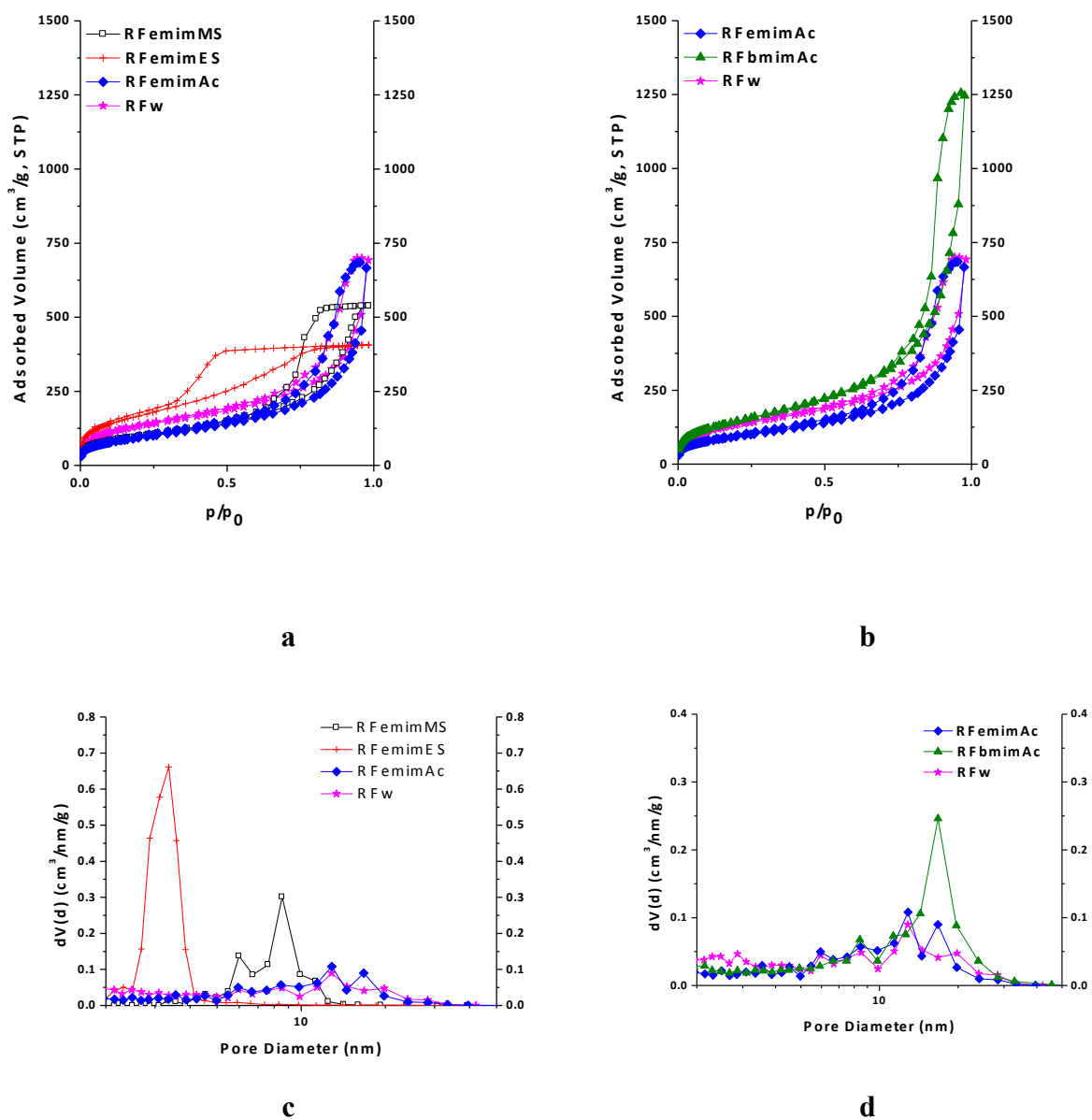


Figure 3 Low temperature (-196 °C) nitrogen adsorption/desorption isotherms of the resorcinol- formaldehyde (RF) polymer gels synthesized in various ionic liquids of the same cation (a) and anion (b) and the corresponding pore size distribution curves from the desorption branch (c, d). The initial water content was ca. 10 wt%. For clarity they are grouped according to ionic composition. The adsorption isotherm obtained in RTIL-free conditions is also included for comparison, in both groups (RFw).

The isotherms and the pore morphology indicate that the polymer – solvent phase separation arising during the polymerization is affected by the nature of the ionic liquid. The structure of

the various systems is very similar. The calculations of Bernardes et al. showed that at $x_{\text{water}} \approx 0.5 - 0.6$, which is the case in the above systems, the water molecules form chain-like structures. We may infer that these structures are influenced by the properties of the ionic liquid [31]. The sample synthesised in 1-ethyl-3-methylimidazolium shows the morphology closest to that in the water medium.

The choice of ionic liquids also allows us to compare the influence of the cations and anions separately. Ion size effects can be observed by inspecting the isotherms synthesized in aqueous mixtures of ionic liquids with 1-ethyl-3-methylimidazolium cations, but with different anions, i.e., in aqueous [emim][Ac], [emim][MeSO₄] and [emim][EtSO₄] solutions (Figure 3 a and c). Costa et al [33] report that the effective molar volumes of methyl sulphate and ethyl sulphate are 73.63 and 91.68 cm³/mol, which correspond to ionic diameters of 0.616 and 0.662 nm, respectively. Consequently, the size of the anions increases in the order acetate < methyl sulphate < ethyl sulphate, and the shape of the isotherm changes accordingly. Polymers synthesized in [emim][Ac] and [emim][MeSO₄] exhibit more limited adsorption in the micropore range than with the bulkier ethyl sulphate anion. The most spectacular is the systematic decrease at the end of the isotherm accompanied by the widening of the hysteresis loop and its transformation into a clearly defined H2a.

Table 4 Data deduced from low temperature gas adsorption and SEM

Sample acronym	$S_{\text{BET}}^{\text{a}}$	$W_{0,\text{DR}}^{\text{b}}$	$V_{\text{TOT}}^{\text{c}}$	$V_{\text{meso}}^{\text{d}}$	$d_{\text{SEM}}^{\text{e}}$
	m ² /g	cm ³ /g	cm ³ /g	cm ³ /g	nm
RFemimMS	352	0.13	0.83	0.70	17 ± 3
RFemimES	608	0.24	0.63	0.39	19 ± 3
RFemimAc	341	0.12	1.03	0.91	21 ± 4
RFbmimAc	391	0.14	1.41	1.27	22 ± 5
RFw	460	0.15	1.07	0.92	19 ± 2

^a Apparent surface area from BET model, ^b Micropore volume from DR method, ^c Pore volume at $p/p_0 \rightarrow 1$, ^d ($V_{\text{TOT}} - W_{0,\text{DR}}$), ^e average diameter of the beads from SEM (based on approx. 100 data)

The closure points of the isotherms shift systematically to smaller p/p_0 values. The systematic modification is reflected in the pore size distribution of Figure 3c. Interestingly, the greater the size of the anion, the lower is the position of the peak, i.e., the pore neck is narrower.

Loops of this type are typical if the pore network consists of macropores that are incompletely filled – in this case with liquid nitrogen. Figures 3 b and d compare the isotherms obtained with ionic liquids having the small acetate anion. Replacing 1-ethyl-3-methylimidazolium by the bulkier 1-butyl-3-methylimidazolium cation results in higher nitrogen uptake over the whole relative pressure range. The spectacular enhancement in the wider mesopore region is responsible for the high total pore volume. The shape of the hysteresis loops, very close to H1, implies that the mesopores have a relatively narrow size distribution, and possibly also an ink-bottle type structure in the interconnected pore system. The wider part of the pores remains filled during desorption until the lower vapour pressures defined by the narrow necks are achieved and allow the pore to empty: they therefore depend on the size and spatial distribution of the necks. The closure point of the hysteresis loop is slightly higher in the case of the larger butyl sulphate. Around this water content the rupture of the polar network is often accompanied by formation of micelles. The butyl chain may be long enough for such self-assembly [44]. The data deduced from the isotherms are listed in **Table 4**. Larger anion size produces a higher surface area, but a lower total pore volume as measured with nitrogen. At the same time, larger cation size leads to both higher surface area and pore volume. The outstanding increase in case of RFbmimAc can be attributed to self-assembly of cations with a relatively long side chain. The systematic shift of the peaks appearing in the desorption branch pore size distribution curves, i.e., the width distribution of the narrowest pore inlets in the mesopore range, is therefore attributable to the size effect of the cations and the anions. This observation introduces a new method of tuning the size of the pore necks that influence the percolation properties of the pore structure.

3.3. Influence of water content

1-Ethyl-3-methylimidazolium ethyl sulphate was selected for the experiments. All the gels for the study below were prepared without added catalyst, i.e., the gelation was driven by the IL itself. The samples and the solvent composition are listed in **Table 5**. As in the previous sections, the highest IL, and thus the lowest water content, was limited by the water added with the formaldehyde.

Table 5 Initial composition of samples synthesized in water (1) – [emim]ES] (2) binary solvent

Sample acronym	Water	IL	R+F	x_{water}
----------------	-------	----	-----	-------------

	wt %			-
RFemimES9	9.1*	75.4	15.5	0.61
RFemimES15	15.4	68.9	15.7	0.75
RFemimES20	19.7	64.4	15.9	0.80
RFemimES25	25.2	58.7	16.1	0.85
RFemimES31	30.9	52.8	16.3	0.89
RFemimES37	36.7	46.8	16.5	0.91
RFemimES43	42.6	40.7	16.7	0.93
RFemimES49	48.7	34.3	16.9	0.95
RFemimES55	55.0	27.8	17.1	0.96

* water content from the formaldehyde solution alone

The SEM images in **Figure 4** show the expected interconnected pore structure of the polymer in the selected samples. Except for sample RFemimES55, where the size of the spherical units is more than two orders of magnitude greater than in any other sample (see also Figure 1), the size of the beads is also very similar. The numerical parameters deduced from the data are listed in **Table 6**.

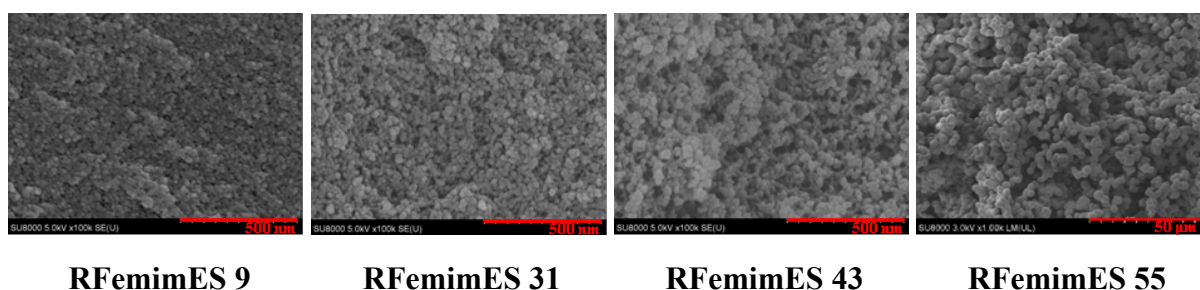
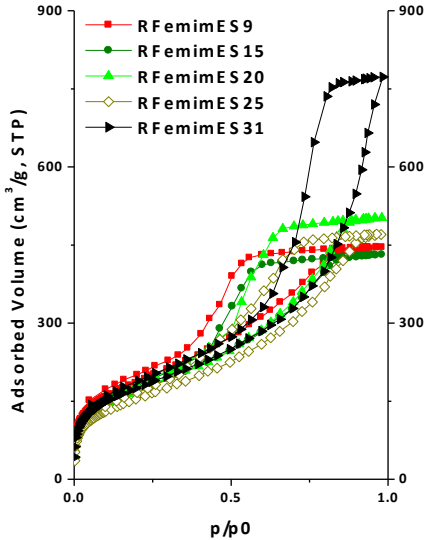


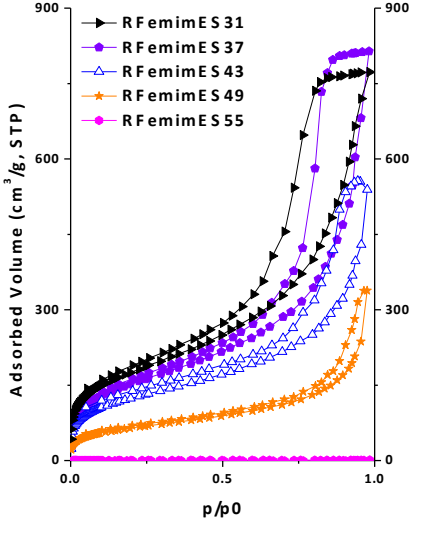
Figure 4. SEM micrographs of selected polymer samples synthesized water (1) – [emim][EtSO₄] (2) binary solvent. Note the larger scale bar in RFemimES55.

For clarity, in both sets of graphs the nitrogen adsorption data are separated into two groups, including RFemimES31. The nitrogen adsorption isotherms (**Figure 5a, b**) appear to differ substantially, but all belong to Type IVa, except for RFemimES55, which shows no measurable adsorption [38]. Some isotherms display limited low pressure hysteresis as well as the expected hysteresis loop in the mesopore range.

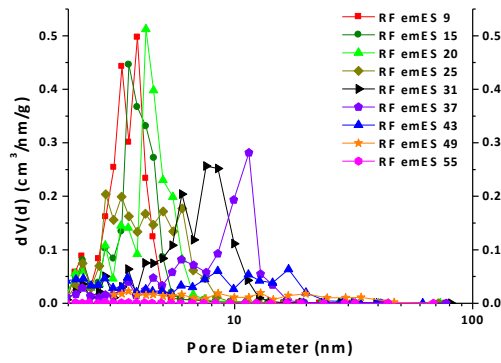
The initially H2(a) type hysteresis loop gradually changes to H1 type and finally to H3. Up to RFemES25 the hysteresis loop implies that the rather complex developing pore structure may be related to a blocking effect by pore necks with a relatively narrow distribution. On increasing the water content, the width of the loop narrows and the contribution to the pore volume of the corresponding pores practically doubles. The H1-like hysteresis loop implies that the pore network being formed under these solvent conditions consists of pores in which the size distribution of the inlets resembles that of the pore itself. Further increase of the water in the binary solvent results in a network of widened pores that also contains macropores incompletely filled with liquid nitrogen. Finally, at $x_1=0.96$ the sample consists only of macropores that are so wide that no nitrogen adsorption is detected, i.e., the sample contains macro- and supermacropores that lie outside the detection range of this technique. According to our experience these samples are too weak to withstand mercury porosimetry, a conclusion that is confirmed by the SEM images. These findings underline the advantage of using the desorption branch to determine the pore size distribution, namely that it yields an estimate of the pore neck size (**Figure 5c**).



a



b



c

Figure 5 Low temperature (-196 °C) nitrogen adsorption/desorption isotherms of the polymer samples (a, b) and synthesized in water (1) – [emim][EtSO₄] (2) mixture and their pore size distribution from the desorption (c) branch in the mesopore range by BJH.

With increasing water content a systematic shift is observed in the position of the peaks, i.e., the most frequent limiting pore width, and also a continuous broadening of the distribution. The apparent surface area and the pore volume from various adsorption models are listed in Table 6. The overall trend in the apparent surface area and the various pore volumes faithfully reflects the changes in pore morphology. Below $x_1=0.85$, the data are unaffected by the water content. The micropore volume is practically constant even up to $x_1\approx 0.90$, as is also the BET surface area. Above 0.85 overall pore widening occurs, as reflected in the sudden increase in the meso- and macropore volumes. Finally, the size of the pores grows beyond the detection window of nitrogen adsorption. Although the mechanical weakness of the polymer matrices excludes the use of mercury porosimetry, the SEM images fully confirm this observation. The typical structure of the polymer aerogels is clearly recognizable in all the SEM images, but the 50 μm scale bar in the case of RFemimES 55 attests to the abrupt change of the size range of the pore network.

Table 6 Data deduced from gas adsorption and SEM observation for the samples synthesized in water (1) – [emim][EtSO₄] (2) binary solvents

Acronym of sample	Molar fraction of water	$S_{\text{BET}}^{\text{a}}$	W_0^{b}	$V_{\text{tot}}^{\text{c}}$	$V_{\text{meso}}^{\text{d}}$	$d_{\text{SEM}}^{\text{e}}$
	-	m^2/g	cm^3/g	cm^3/g	cm^3/g	nm
RFemES 9	0.61	674	0.24	0.69	0.45	16 ± 3

RFemES 15	0.75	603	0.22	0.67	0.45	n.a.
RFemES 20	0.80	606	0.23	0.77	0.54	n.a.
RFemES 25	0.85	558	0.22	0.72	0.50	n.a.
RFemES 31	0.89	634	0.25	1.12	0.87	16 ± 4
RFemES 37	0.91	543	0.21	1.26	1.05	n.a.
RFemES 43	0.93	452	0.18	0.83	0.65	22 ± 4
RFemES 49	0.95	232	0.09	0.52	0.43	n.a.
RFemES 55	0.96	0	0	0	0	2913 ± 217

^a Apparent surface area from BET, ^b Micropore volume from DR, ^c Pore volume at $p/p_0 \rightarrow 1$, ^d $V_{\text{tot}} - W_0$, ^e average diameter of the beads from SEM (based on approx. 100 data). n.a.: not available

The set of samples described above demonstrates that a metal-free ionic liquid medium is also able to generate suitable conditions for the sol-gel process of resorcinol and formaldehyde.

At ambient temperature the water (1) – 1-ethyl-3-methylimidazolium ethyl sulphate (2) system, which was used to study the effect of composition, is completely miscible. The density, dynamic viscosity and surface tension of this binary solvent as a function of water molar fraction, from the experimental data of Gomez et al. [29] and Fröba et al. [30], are plotted in **Figure 6**. Both sets of measurements were obtained on non-commercial RTIL samples. In the concentration range explored in our work (designated by arrows in the figure) both the density and the surface tension display strong non-linearity, while the dynamic viscosity varies only weakly. The similarity between the behaviour of the density and surface tension of the water – IL mixtures on the one hand, and both the surface area and pore volume of the polymer aerogels on the other (Figure 6d), reinforces the idea that the growth of the gel structure is driven by the spatial structure of the solvent mixture and thus is an indicator of its thermodynamics.

The synthesis of the samples, however, was performed not at ambient temperature but at 85 °C. At elevated temperature only limited information is available on the physicochemical properties of water (1) – 1-ethyl-3-methylimidazolium ethyl sulphate (2) binary mixtures. Gomez et al. [29], who studied this water-ionic liquid system up to 55 °C, showed that at 25 °C the excess molar volume of the mixture, which is U-shaped and everywhere negative, gradually transforms to an S-shape at temperatures above 35 °C. In the range $0 < x_1 < 0.8$ the excess volume thus remains negative, but at higher water content ($x_1 \approx 0.9$) it turns positive,

with a maximum that increases strongly with increasing temperature, signaling a trend towards phase separation.

The change in internal structure of the water (1) – 1-ethyl-3-methylimidazolium ethyl sulphate (2) mixture with composition is corroborated by the molecular dynamics (MD) calculations of Bernardes et al. [31]. At 25 °C these authors identify three different structural systems in the concentration range spanned in our synthesis. At low water content, up to $x_I \approx 0.5$ the ionic liquid forms a polar network. In the range $0.5 < x_I < 0.8$ this network starts to be replaced by chain-like water clusters, while in the range $0.8 < x_I < 0.95$ the mixture is bi-continuous. The percolation limit of water is reached at $x_I=0.95$, above which the ionic liquid network collapses into isolated solvated ions or small clusters of ions. Although the breakdown of the polar network could be accompanied by the formation of micelles, the ethyl side-chains are not long enough to achieve this self-assembly. [31] The two distinct percolation limits for water in the ionic liquid network and ionic liquid in water set by this model calculation, namely $x_I \approx 0.8$ and $x_I \approx 0.95$, respectively, show notably good agreement with our experimental observations, in spite of the presence of the other components in the synthesis mixture. The bi-continuous region gives rise to an exclusively super-macroporous structure in which nitrogen adsorption is unable to detect pores. At more elevated temperatures it seems likely that the solubility conditions tend to be even less favourable, giving rise to the outstandingly large bead and pore sizes. As has already been noted by Svec, poor miscibility gives rise to wider pores [45]. Our results thus show that adjusting the water content of the binary solvent phase provides a novel means of tuning the pore morphology of these polymer aerogels.

Although all these phenomena may contribute to the mechanism and the kinetics of the gelation, as might be concluded from the comparison of shapes of the curves in Fig. 6, our results indicate that the most important factor is the dilution of the reaction mixture from sample RFemES 9 to RFemES 55. A significant observation is that in the range $x_I = 0.61$ to $x_I = 0.96$ the pH changes from 9.2 to 7.7, but it always remains in the basic zone. It is widely known that changing the concentration of the catalyst is a means of tuning the morphology: larger concentration yields smaller beads and a more compact system, while smaller amounts of catalyst lead to larger beads and a looser structure [46]. These observations show that 1-ethyl-3-methylimidazolium ethyl sulphate acts as nucleation centre and its concentration decreases with increasing water content.

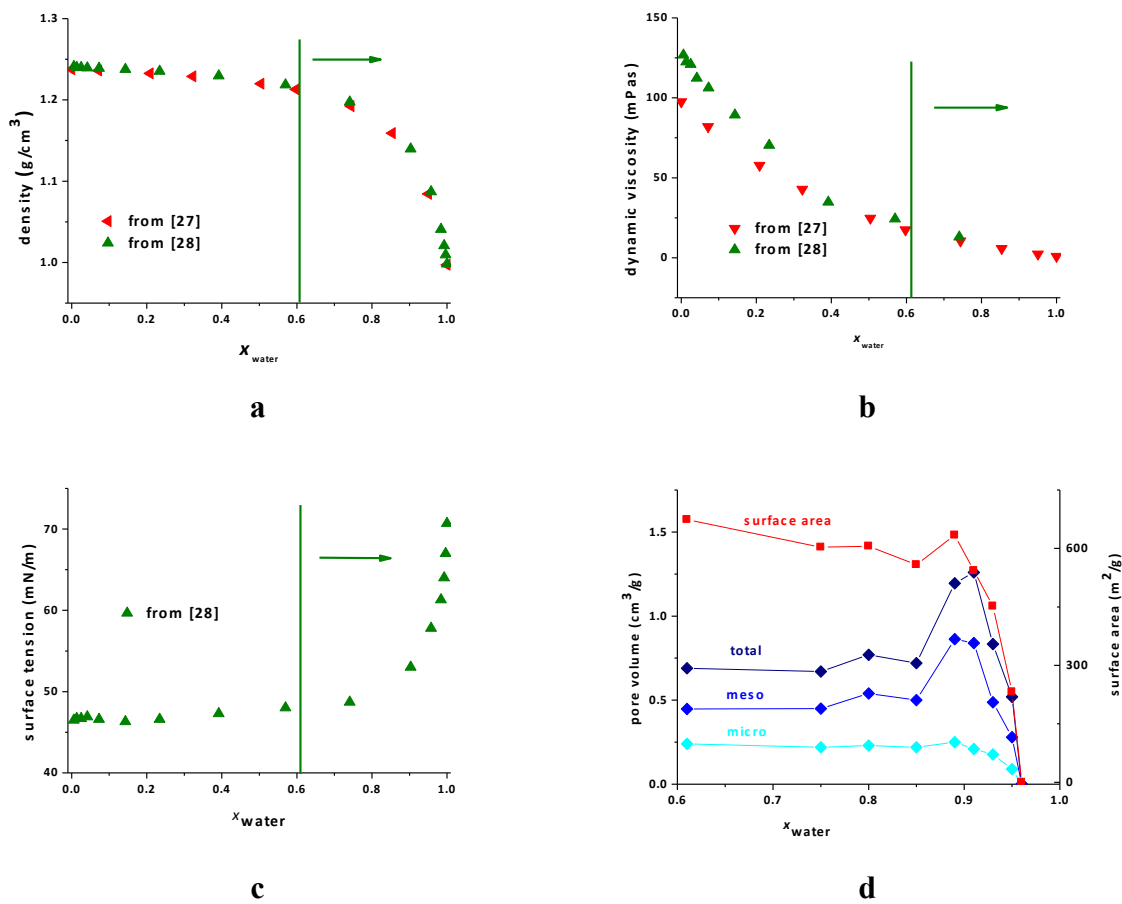


Figure 6 Influence of dilution on various physico-chemical properties of water (1) - [emim][EtSO₄] (2) binary mixtures. (a) density, (b) dynamic viscosity; (c) surface tension. From Refs. [29] at 25 °C and [30] at 20 °C. The green line and arrow delimit the concentration range used in our study. (d) morphological characteristics of the polymer aerogels.

Although the experimental evidence presented here demonstrates the parallel between changes in the structure of the mixed solvent and the influence of the water content on the sol/gel process, the major driving force is the concentration of the nucleating effect of the basic ionic liquid. An understanding of the driving force and the detailed mechanism of these structural changes calls for further experimental and modelling work, notably in the elevated temperature range.

4. Conclusions

Ionic liquids can play a twofold role in the sol/gel synthesis of resorcinol – formaldehyde based polymer gels. They are an excellent recyclable porogen and in certain cases also act as a

metal free catalyst, thus providing a truly metal-free carbon precursor polymer. Our systematic study with carefully selected room temperature ionic liquid groups of identical cations or anions reveals that both the anions and the cations impact the structure formation. The nitrogen adsorption isotherms reveal that the influence of the anions is more pronounced in the lower relative pressure range (development of smaller pores), while the cations affect the morphology of the wider pores. Binary mixtures of water – 1-ethyl-3-methylimidazolium ethyl sulphate ionic liquid of systematically adjusted molar composition enable us to explore their potential in tuning the morphology of the dried ionogels. An unexpected finding in these systems is that no additional catalyst is necessary for the synthesis, a result that appears to be attributable to the intrinsically basic nature of imidazolium type ILs with the ethyl and methyl sulphate anions. A radical effect occurs at the water – ionic liquid molecular ratio 96:4, where the size of the elementary building beads suddenly grows by two orders of magnitude. These findings can be considered as experimental evidence of changes in the solvent structure that are consistent with the molecular dynamics simulations of Bernardes [31]. To understand the driving force and the detailed mechanism of the structural changes observed, however, requires further experimental and modelling work, notably in the elevated temperature range.

Acknowledgement

The authors are grateful to Prof. P. Huszthy for fruitful discussions, to J. Madarász for TG/MS measurements and to E. Székely for her valuable contribution to supercritical drying. We thank Gy. Bosznai for his technical assistance. Financial support from the Hungarian Scientific Research Fund NN123631 and VEKOP-2.3.2-16-2017-00013 is acknowledged. The VEKOP project is supported by the EU and by Hungary, co-financed by the European Regional Development Fund. The work is also part of the EU project NANOMED (H2020-MSCA-RISE-2016, #734641). The research reported in this paper was supported by the BME-Biotechnology FIKP grant of EMMI (BME FIKP-BIO).

References

- [1] D. Wu, F. Xu, B. Sun, R. Fu, H. He, K. Matyjaszewski: Design and Preparation of Porous Polymers. *Chemical Review* 2012; 112(7): 3959-4015. <https://doi.org/10.1021/cr200440z>
- [2] V. M. Gun'ko, I.N. Savina, S. V. Mikhalovsky: Cryogels: Morphological, structural and adsorption characterisation. *Advances in Colloid and Interface Science* 2013; 187-188: 1-46. <https://doi.org/10.1016/j.cis.2012.11.001>

- [3] B. Gyarmati, E. Z. Mészár, L. Kiss, M. A. Deli, K. László, A. Szilágyi: Supermacroporous chemically cross-linked poly(aspartic acid) hydrogels. *Acta Biomaterialia* 2015; 22: 32-38. <https://doi.org/10.1016/j.actbio.2015.04.033>
- [4] E. Manek, B. Berke, N. Miklósi, M. Sajbán, A. Domán, T. Fukuda, O. Czakkel, K. László: Thermal sensitivity of carbon nanotube and graphene oxide containing responsive hydrogels. *Express Polymer Letters* 2016; 10(8): 710–720. <https://doi.org/10.3144/expresspolymlett.2016.64>
- [5] J. Wu, F. Xu, S. Li, P. Ma, X. Zhang, Q. Liu, R. Fu, D. Wu: Porous Polymers as Multifunctional Material Platforms toward Task-Specific Applications. *Advanced Materials* 2019; 31: 1802922. <https://doi.org/10.1002/adma.201802922>
- [6] A. Arenillas, J. A. Menéndez, G. Reichenauer, A. Celzard, V. Fierro, F. J. Maldonado-Hodar, E. Bailón-García, N. Job: Organic and Carbon Gels. From Laboratory Synthesis to Applications Organic and Carbon Gels: From Laboratory to Industry. Book Series: Advances in Sol-Gel Derived Materials and Technologies. Springer, 2019
- [7] R. W. Pekala: Organic aerogels from the polycondensation of resorcinol with formaldehyde. *Journal of Materials Science* 1989; 24: 3221-3227. <https://doi.org/10.1007/BF01139044>
- [8] B. Singco, C. L. Lin, Y. J. Cheng, Y.H. Shih, H.Y Huang: Ionic liquids as porogens in the microwave-assisted synthesis of methacrylate monoliths for chromatographic application. *Analytica Chimica Acta* 2012; 746: 123– 133. <http://dx.doi.org/10.1016/j.aca.2012.08.034>
- [9] O. Czakkel, K. Marthi, E. Geissler, K. László: Influence of Drying on the Morphology of Resorcinol - Formaldehyde-based Carbon Gels. *Microporous and Mesoporous Materials* 2005; 86(1-3): 124-133. doi:10.1016/j.micromeso.2005.07.021
- [10] B. Nagy, I. Bakos, I. Bertóti, A. Domán, A. Menyhárd, M. Mohai, K. László: Synergism of melamine and GO in the electrocatalytic behaviour of resorcinol - formaldehyde based carbon aerogels. *Carbon* 2018; 139: 872-879. <https://doi.org/10.1016/j.carbon.2018.07.061>
- [11] B. Nagy, A. Domán, A. Menyhárd, K. László: Influence of Graphene Oxide Incorporation on Resorcinol-Formaldehyde Polymer and Carbon Aerogels. *Periodica Polytechnica Chemical Engineering* 2018; 62(4), 441-449. <https://doi.org/10.3311/PPch.12915>.
- [12] R. Hayes, G. G. Warr, R. Atkin: Structure and Nanostructure in Ionic Liquids. *Chemical Review* 2015; 115: 6357–6426. <https://doi.org/10.1021/cr500411q>

- [13] Q. G. Zhang, N. N. Wang, Z.W. Yu: The Hydrogen Bonding Interactions between the Ionic Liquid 1-Ethyl-3-Methylimidazolium Ethyl Sulfate and Water. *Journal of Physical Chemistry B* 2010; 114: 4747–4754. <https://doi.org/10.1021/jp1009498>
- [14] J. Lu, F. Yan, J. Texter: Advanced applications of ionic liquids in polymer science. *Progress in Polymer Science* 2009; 34: 431–448. <https://doi.org/10.1016/j.progpolymsci.2008.12.001>
- [15] J. Wang, X. Jiang, H. Zhang, S. Liu, L. Bai, H. Liu: Preparation of a porous polymer monolithic column with an ionic liquid as a porogen and its applications for the separation of small molecules in high performance liquid chromatography. *Analytical Methods* 2015; 7: 7879–7888. <https://doi.org/10.1039/c5ay01487e>
- [16] T. Ogoshi, T. Onodera, T.A. Yamagishi, Y. Nakamoto, A. Kagata, N. Matsumi, K. Aoi: Transparent ionic liquid-phenol resin hybrids with high ionic conductivity. *Polymer Journal* 2011; 43: 421-424. <https://doi.org/10.1038/pj.2011.1>
- [17] W. Zhang, T. Liu, H. Wu, P. Wu, M. He, Direct synthesis of ordered imidazolyl-functionalized mesoporous polymers for efficient chemical fixation of CO₂. *Chem. Commun.* 2015; 51: 682-684.
- [18] A. Chen; Y. Li, L. Liu, Y. Yu, K. Xia, Y. Wang, S. Li: Controllable synthesis of nitrogen-doped hollow mesoporous carbon spheres using ionic liquids as template for supercapacitors. *Applied Surface Science* 2017; 393: 151-158. <http://dx.doi.org/10.1016/j.apsusc.2016.10.025>
- [19] H. Yang, X. Cui, Y. Deng, F. Shi, Ionic liquid templated preparation of carbon aerogels based on resorcinol–formaldehyde: properties and catalytic performance. *Journal of Materials Chemistry* 2012; 22(41): 21852-21856. <https://doi.org/10.1039/C2JM35258C>
- [20] Z. Ling, G. Wang, Q. Dong, B. Qian, M. Zhang, C. Li, J. Qiu: An ionic liquid template approach to graphene–carbon xerogel composites for supercapacitors with enhanced performance. *Journal of Materials Chemistry A* 2014; 2(35):14329-14333. <https://doi.org/10.1039/C4TA02223H>
- [21] W. Zhang, Q. Wang, H. Wu, P. Wu, M. He, A highly ordered mesoporous polymer supported imidazolium-based ionic liquid: an efficient catalyst for cycloaddition of CO₂ with epoxides to produce cyclic carbonates. *Green Chem.* 2014; 16: 4767-4774.
- [22] Z.L. Xie, R. J. White, J. Weber, A. Taubert, M. M Titirici: Hierarchical porous carbonaceous materials via ionothermal carbonization of carbohydrates. *Journal of Materials Chemistry* 2011; 21: 7434–7442. <https://doi.org/10.1039/C1JM00013F>

- [23] Y.Y. Yao, T. Zhou, T. Yang, R.L. Xiang, Y.R. Wu: Homogeneous thermal stabilization of polyacrylonitrile in an ionic liquid solution for the production of carbon nanosphere. *Carbon* 2013; 58: 249–251. <https://doi.org/10.1016/j.carbon.2013.02.060>
- [24] J.S. Lee, R.T. Mayes, H.M. Luo, S. Dai, Ionothermal carbonization of sugars in aprotic ionic liquid under ambient conditions. *Carbon* 2010; 48: 3364–3368. <https://doi.org/10.1016/j.carbon.2010.05.027>
- [25] J.S. Lee, X.Q. Wang, H.M. Luo, G.A. Baker, S. Dai: Facile ionothermal synthesis of microporous and mesoporous carbons from task specific ionic liquids. *Journal of American Chemical Society* 2009; 131: 4596–4597. <https://doi.org/10.1021/ja900686d>
- [26] Z. Zhang, G. M. Veith, G. M. Brown, P. F. Fulvio, P. C. Hillesheim, S. Dai, S. H. Overbury: Ionic liquid derived carbons as highly efficient oxygen reduction catalysts: first elucidation of pore size distribution dependent kinetics. *Chemical Communications* 2014; 50: 1469–1471. <https://doi.org/10.1039/C3CC48942F>
- [27] X.J. Bo, J. Bai, J. Ju, L.P. Guo: Highly dispersed Pt nanoparticles supported on poly(ionic liquids) derived hollow carbon spheres for methanol oxidation. *Journal of Power Sources* 2011; 196: 8360–8365. <https://doi.org/10.1016/j.jpowsour.2011.06.068>
- [28] Y. Ma, G. Ji, B. Ding, J.Y. Lee: N-doped carbon encapsulation of ultrafine silicon nanocrystallites for high performance lithium ion storage, *Journal of Materials Chemistry A* 2013; 1: 13625–13631. <https://doi.org/10.1039/C3TA13268D>
- [29] E. Gomez, B. Gonzalez, N. Calvar, E. Tojo, A. Dominguez: Physical Properties of Pure 1-Ethyl-3-methylimidazolium Ethylsulfate and Its Binary Mixtures with Ethanol and Water at Several Temperatures. *Journal of Chemical Engineering Data* 2006; 51: 2096-2102. <https://doi.org/10.1021/je060228n>
- [30] A. P. Fröba, P. Wasserscheid, D. Gerhard, H. Kremer, A. Leipertz: Revealing the Influence of the Strength of Coulomb Interactions on the Viscosity and Interfacial Tension of Ionic Liquid Cosolvent Mixtures. *Journal of Physical Chemistry B* 2007; 111: 12817-12822. <https://doi.org/10.1021/jp074799d>
- [31] C. E. S. Bernardes, M. E. Minas da Piedade, J. N. C. Lopes: The Structure of Aqueous Solutions of a Hydrophilic Ionic Liquid: The Full Concentration Range of 1-Ethyl-3-methylimidazolium Ethylsulfate and Water. *Journal of Physical Chemistry B* 2011; 115: 2067–2074. <https://doi.org/10.1021/jp1113202>
- [32] Y. Kohno, Hiroyuki Ohno: Ionic liquid/water mixtures: from hostility to conciliation. *Chemical Communications* 2012; 48: 7119–7130. <https://doi.org/10.1039/C2CC31638B>

- [33] A. J. L. Costa, J. M. S. S. Esperança, I. M. Marrucho, L. P. N. Rebelo: Densities and Viscosities of 1-Ethyl-3-methylimidazolium n-Alkyl Sulfates. *Journal of Chemical Engineering Data* 2011; 56: 3433–3441. <https://doi.org/10.1021/je200434a>
- [34] <https://www.sigmaaldrich.com/catalog>. Last visited 24 May 2019
- [35] <https://www.chemicalbook.com>. Last visited 24 May 2019
- [36] S. J. Taylor, M. D. Haw, J. Sefcik, A. J. Fletcher: Gelation Mechanism of Resorcinol-Formaldehyde Gels Investigated by Dynamic Light Scattering. *Langmuir* 2014; 30: 10231–10240. <https://doi.org/10.1021/la502394u>
- [37] M. Reuss, L. Ratke: RF-aerogels catalysed by ammonium carbonate. *J. Sol - Gel Sci Technol* 2010; 53:85-92. <https://doi.org/10.1007/s10971-009-2060-9>
- [38] M. Thommes, K. Kaneko, A. V. Neimark, J. P. Olivier, F. Rodriguez-Reinoso, J. Rouquerol, K. S. W. Sing: Physisorption of gases, with special reference to the evaluation of surface area and pore size distribution (IUPAC Technical Report). *Pure and Applied Chemistry* 2015; 87(9-10): 1051–1069. <https://doi.org/10.1515/pac-2014-1117>
- [39] Lin C., Ritter J.A.: Effect of synthesis pH on the structure of carbon xerogels. *Carbon* 1997; 35: 1271-1978.
- [40] N. Job, F. Panariello, J. Marien, M. Crine, J.P. Pirard, A. Léonard A.: Synthesis optimization of organic xerogels produced from convective air-drying of resorcinol-formaldehyde gels. *Journal of Non-Crystalline Solids* 2006; 352: 24-34.
- [41] N. Job N, R. Pirard, J. Marien, J.P Pirard: Porous carbon xerogels with texture tailored by pH control during sol-gel process. *Carbon* 2004; 42: 619-628.
- [42] Binshen Wang, Li Qin, Tiancheng Mu, Zhimin Xue, Guohua Gao: Are Ionic Liquids Chemically Stable? *Chem. Rev.* 2017; 117: 7113–7131.
- [43] V. K. Aggarwal, I. Emme, A. Mereu: Unexpected Side Reactions of Imidazolium-Based Ionic Liquids in the Base-Catalysed Baylis–Hillman Reaction. *Chem. Commun.* 2002; 1612–1613.
- [44] H.-W. Cheng, J.-N. Dienemann, P. Stock, C. Merola, Y.-J. Chen, M. Valtiner: The Effect of Water and Confinement on Self-Assembly of Imidazolium Based Ionic Liquids at Mica Interfaces. *Scientific Reports* 2016; 6:30058. DOI: 10.1038/srep30058
- [45] F. Svec, J.M.J. Frechet: Kinetic Control of Pore Formation in Macroporous Polymers. Formation of "Molded" Porous Materials with High Flow Characteristics for Separations or Catalysis. *Chemistry of Materials* 1995; 7: 707–715. <https://doi.org/10.1021/cm00052a016>

[46] T. Yamamoto, T. Nishimura, T. Suzuki, H. Tamon: Control of mesoporosity of carbon gels prepared by sol–gel polycondensation and freeze drying. *Journal of Non-Crystalline Solids* 2001; 288: 46–55.